MEASUREMENT OF SYNCHRONIZATION IN NOISY AND CHAOTIC DYNAMICAL SYSTEMS

by

P. Khoury, M. A. Lieberman, and A. J. Lichtenberg

Memorandum No. UCB/ERL M95/103

22 December 1995

MEASUREMENT OF SYNCHRONIZATION IN NOISY AND CHAOTIC DYNAMICAL SYSTEMS

by

P. Khoury, M. A. Lieberman, and A. J. Lichtenberg

Memorandum No. UCB/ERL M95/103

22 December 1995

ELECTRONICS RESEARCH LABORATORY

College of Engineering
University of California, Berkeley
94720

Measurement of synchronization in noisy and chaotic dynamical systems

P. Khoury, M. A. Lieberman, and A. J. Lichtenberg

Department of Electrical Engineering and Computer Sciences, and the Electronics Research Laboratory, University of California, Berkeley, CA 94720, USA

The degree of synchronization of two nearly-identical response subsystems with noisy input is characterized through use of two different measures: the conditional lyapunov exponent and the distribution exponent. The conditional lyapunov exponent describes the stability of the subsystem, and the distribution exponent describes the probability of separation of the two subsystems. A simple piecewise linear map illustrates the continuous nature of synchronization and shows the benefits and significance of each measure. The conditional lyapunov exponent is more easily calculated than the distribution exponent, but the distribution exponent seems more physically descriptive of synchronization. An important correspondence, that both measures cross through zero at the same time, is proved.

PACS number: 05.45.+b, 02.50.Ey

I. INTRODUCTION

Pecora and Carroll made widely known the possibility of chaotic synchronization [1,2,3]. The systems in which one usually observes chaotic synchronization are two duplicate response subsystems fed with a common chaotic drive signal [4, 5,6,7].

Chaotic synchronization occurs when, after an initial transient period, the outputs of the response subsystems evolve in an identical fashion despite having different initial conditions. The entire system, drive and response systems, can either be described with differential equations or mapping equations. In this paper we use mapping equations for all of our examples, which can be described by the following vector equations:

$$\begin{aligned} v_{i+1} &= f(v_i, u_i) && \text{drive variable} \\ u_{i+1} &= g(v_i, u_i) && \text{rest of the drive system} \\ w_{i+1} &= h(v_i, w_i) && \text{response subsystem} \\ x_{i+1} &= h(v_i, x_i) && \text{duplicate response subsystem} \end{aligned} \tag{1}$$

Synchronization occurs when, for arbitrary initial conditions,

$$\lim_{i\to\infty} |w_i - x_i| = 0. \tag{2}$$

The conditional lyapunov multipliers of the response subsystem must be less than zero for synchronization to occur [1]. Using spec to represent the spectrum of eigenvalues [8] and D_w to represent the Jacobian of a function with respect to the variable w, this condition can be written:

$$\text{spec}\left[\prod_{i=1}^{\infty} D_w h(v_i, w_i)\right] < 0. \tag{3}$$

Many researchers have considered applying chaotic synchronization to the practical realm of secure communication. If a receiver and transmitter are synchronized and behave chaotically, perhaps information can be sent with a low probability of intercept [9, 10]. All the studies of chaotic synchronization and its application have treated the phenomenon as a binary one, i.e. systems are either synchronized or not synchronized. In this work we show that synchronization is a continuous phenomena; systems have a degree of synchronization. By changing a parameter one can make a response subsystem more synchronized than before. Quantifying the phenomenon of chaotic synchronization is fundamental to understanding it and using it in applications.

One obvious measure of synchronization is the value of the conditional lyapunov exponent. We use this measure in the example that we explore; but we also introduce another measure, the distribution exponent. As its name implies, the distribution exponent is the characteristic geometric exponent of the probability distribution of the separation between two nearly identical response subsystems. This measure was introduced in a paper by Pikovsky [11], and we use many of his ideas here. To a large extent, this second measure captures the concept of degree of synchronization better than the conditional lyapunov exponent. Each measure offers different insights, and one or the other might be more useful in a particular situation. In this paper we study the correspondence between the two measures.

In this work we study synchronization in response subsystems driven by additive random noise rather than by deterministic chaotic noise; however the analogy between the two is obvious. Our simple comparisons through computer simulation between noisy and chaotic synchronization confirm the analogy by indicating that qualitative findings discovered about noisy synchronization can be applied to chaotic synchronization.

II. ANALYSIS AND NUMERICAL COMPARISONS

The basic system used for illustration in this paper is two maps with additive noise

$$\begin{aligned} w_{n+1} &= h(w_n) + \theta_n \\ x_{n+1} &= h(x_n) + \vartheta_n \end{aligned} \quad . \tag{4}$$

The random processes θ and ϑ are almost identical. The two processes differ slightly for reasons that will become clear as the distribution exponent is explained. These random processes can be split into a common component ξ and an asymmetric component δ

$$\begin{aligned} \theta_n &= \xi_n + \tfrac{\delta_n}{2} \\ \vartheta_n &= \xi_n - \tfrac{\delta_n}{2} \end{aligned} \quad . \tag{5}$$

The standard deviation of the asymmetric component is assumed to be orders of magnitude less than the standard deviation of the system variable x. Substituting (5) in (4) we obtain the system for study in this paper

$$\begin{aligned} w_{n+1} &= h(w_n) + \xi_n + \tfrac{\delta_n}{2} \\ x_{n+1} &= h(x_n) + \xi_n - \tfrac{\delta_n}{2} \end{aligned} . \tag{6}$$

Equations (6) can be transformed by introducing the sum and difference variables

$$\begin{aligned} s_n &= \frac{w_n + x_n}{2} \\ r_n &= w_n - x_n \end{aligned} . \tag{7}$$

The distribution exponent and the analysis leading up to it will only apply for r small. As our analysis proceeds it will become obvious why this is not a significant restriction. Later we will also make general arguments about the behavior of r when r grows large. Since r is assumed to be small the expressions for $h(w)$ and $h(x)$ can be approximated with a Taylor expansion:

$$\begin{aligned} h(w_n) &= h(s_n + \tfrac{r_n}{2}) \approx h(s_n) + h'(s_n)\tfrac{r_n}{2} \\ h(x_n) &= h(s_n - \tfrac{r_n}{2}) \approx h(s_n) - h'(s_n)\tfrac{r_n}{2} \end{aligned} . \tag{8}$$

Substituting these expressions into equations (6) and adding and subtracting the two equations gives

$$s_{n+1} = h(s_n) + \xi_n \tag{9}$$

$$r_{n+1} = h'(s_n) r_n + \delta_n . \tag{10}$$

The sum variable is now decoupled from the difference variable, and the difference variable depends in a simple way on the sum variable.

A. Sum Equation for a Linear Map

We examine equation (9) first, for linear maps $h(s)=ms$ and different types of noise ξ. A simple linear mapping, $s_{n+1} = ms_n$, becomes unstable for $|m| > 1$. This also holds for a linear mapping with additive noise $s_{n+1} = ms_n + \xi_n$. When $|m| > 1$, a particular noise contribution becomes larger with each iteration, and the variable s will not remain

bounded for long times. Hence we examine the case where $|m| < 1$. Additionally, we assume that the process is white noise, so that subsequent time steps are independent. Because the distribution of the sum of two independent random variables is the convolution of the two distributions, the convolution of the distribution of $h(s_n)$ with the distribution of ξ gives the distribution of s_{n+1}. Therefore, if the distribution S of s is to remain invariant it must satisfy the equation

$$S(s) = \frac{1}{m}\int_{-\infty}^{\infty} \Xi(s - s')S(\frac{s'}{m})ds' . \tag{11}$$

Where Ξ is the distribution of ξ and m is the slope of the linear map.

The solution of this equation is straightforward if the distribution Ξ is gaussian. We then know that S is gaussian, because two gaussian distributions convolved with each other give another gaussian distribution. An odd mapping, $h(x) = -h(-x)$ and the even distribution of Ξ produce an even distribution S that has mean zero. Since we know the form of the distribution is gaussian with mean zero, the variance of the distribution is the last parameter needed to fully specify the distribution. A self consistency approach can be used to determine the variance. (This variance analysis applies to any and all distributions of the additive noise; however the form of the invariant distribution of s will not be the same as the distribution of ξ, and will almost surely not be a simple function if the distribution of ξ is not gaussian.) Because the mean of s is zero the variance and the second moment are equal, and for (11) to hold the second moment of s_{n+1} must equal the second moment of s_n

$$\mathsf{E}(s_{n+1}^2) = \mathsf{E}(s_n^2). \tag{12}$$

Substituting the linear version of (9) into (12) we have

$$\mathsf{E}((ms + \xi)^2) = \mathsf{E}(s^2). \tag{13}$$

Invoke the independence of s and ξ to produce

$$m^2\mathsf{E}(s^2) + \mathsf{E}(\xi^2) = \mathsf{E}(s^2). \tag{14}$$

Solve for $\mathsf{E}(s^2)$

$$\mathbf{E}(s^2) = \frac{\mathbf{E}(\xi^2)}{1-m^2}. \tag{15}$$

Note that the second moment, $\mathbf{E}(s^2)$, and thus the variance of the distribution S is proportional to the variance of the noise distribution Ξ. The variance is singular at $m=\pm 1$.

Two extremes of the linear map, $m=0$ and $m=1$, are easy to analyze analytically for any noise distribution. Any map with slope $m=0$ simply reduces to an identity between s and ξ

$$s_{n+1} = \xi_n. \tag{16}$$

Thus at zero slope, s will be distributed exactly identically to the random variable. As the slope nears 1 the variance of s increases. At slope $m=1$, s_N becomes a direct sum of N independent random variables drawn from the process ξ,

$$\begin{aligned} s_0 &= 0 \\ s_N &= \sum_{n=0}^{N-1} \xi_n \end{aligned} \tag{17}$$

The variance of this sum diverges as N where N is the number of terms in the sum. The central limit theorem states that this sum of independent identically distributed random variables rescaled by N will approach a normal distribution as N approaches infinity . Hence for $m=0$ the distribution is given by the distribution of the random variable itself; and for $m=1$ the distribution approaches a gaussian. For intermediate slopes one gets interesting behavior. As m increases from 0 to 1 the distribution of s changes from the noise distribution ξ to a broad gaussian. In these intermediate regimes fractal distributions of s can result from discrete distributions of ξ.

B. Sum Equation for a Piecewise Linear Map

The ideas of self consistency developed in equations (12,13,14,15) can be extended to some piecewise linear maps by considering a gaussian noise distribution of ξ with mean zero. The maps chosen are odd so that the mean of the invariant distribution remains zero. The maps are also chosen so that the transformation of any gaussian

distribution by the map results in a new distribution with a single maximum. We approximate the new transformed distribution with a gaussian distribution having the same variance as the new transformed distribution. Using self consistency ideas, the variance of the invariant distribution is the same after having applied the map and added the noise as it was before. Starting from (12) and substituting in (9), we have

$$\mathsf{E}((h(s)+\xi)^2)=\mathsf{E}(s^2). \tag{18}$$

Since s and ξ are independent (18) can be transformed to

$$\mathsf{E}(h(s)^2)+\mathsf{E}(\xi^2)=\mathsf{E}(s^2). \tag{19}$$

We determine $\mathsf{E}(h(s^2))$ by assuming that s is gaussian distributed with mean zero and variance $\mathsf{E}(s^2)$ and compute the variance of the new transformed distribution, $h(s)$. We check these assumptions by comparing analytic results with computer simulations for a simple map. Consider the piecewise linear map which is 0 from -1 to 1 and slope 1/2 everywhere else. The noise added to the map has unity variance. Equation (19) solved on a computer predicts that the variance of the invariant distribution will be 1.04097, while after a computer simulation of 5×10^7 iterations of the map, the variance was calculated to be 1.041. Figure 1 shows the invariant distribution and the error between the gaussian distribution with variance calculated using (19) and a distribution estimated from a computer simulation of 5×10^7 iterations.

C. Difference Equation

Equation (10) describes the dynamics of the separation between the two subsystems. Following the work of Pikovsky [11], we first ignore the difference noise δ and look at a logarithmic transformation of (10)

$$z_n=\ln|r_n| \tag{20}$$

giving

$$z_{n+1}=z_n+\ln|h'(s_n)|. \tag{21}$$

The quantity $\ln|h'(s_n)|$ is an instantaneous lyapunov exponent because it describes the change in the separation of two nearby maps over a single time step. We gather the instantaneous exponents together in groups of N and average those groups to get what we call a running average lyapunov exponent

$$\Lambda_j^N = \frac{1}{N}\sum_{n=j}^{j+N-1}\ln|h'(s_n)|. \tag{22}$$

Pikovsky calls these running averages local lyapunov exponents because they are local in time. The evolution of the difference variable can now be described using running average lyapunov exponents

$$z_{N(i+1)} = z_{Ni} + N\Lambda_{Ni}^N. \tag{23}$$

We assume that adjacent running average lyapunov exponents, Λ_{Ni}^N and $\Lambda_{N(i+1)}^N$, become independent of each other as N grows large because the correlation between adjacent running averages decreases as the group size grows. With this assumption their sum follows central limit theorem behavior. In addition we assume that z and Λ_{Ni}^N become independent for large N. In simulations we have found that the correlation decreases between the two variables as N increases, which justifies this assumption. Therefore the invariant distribution Z for z satisfies

$$Z_{N(i+1)}(z) = \int_{-\infty}^{\infty} L^N(\Lambda^N) Z_{Ni}(z - N\Lambda^N)\, d\Lambda^N, \tag{24}$$

where $L^N(\Lambda^N)$ is the invariant distribution of the running average lyapunov exponents normalized such that

$$\int_{-\infty}^{\infty} L^N(\Lambda^N)\, d\Lambda^N = 1. \tag{25}$$

The form of Z that satisfies this equation is

$$Z_{Ni}(z) = e^{\sigma z}. \tag{26}$$

Inserting (26) into equation (24) gives an expression for σ

$$e^{\sigma z} = \int_{-\infty}^{\infty} L^N(\Lambda^N) e^{\sigma(z - N\Lambda^N)} d\Lambda^N \tag{27}$$

or

$$1 = \int_{-\infty}^{\infty} L^N(\Lambda^N) e^{-\sigma N\Lambda^N} d\Lambda^N . \tag{28}$$

If $L^N(\Lambda^N)$ is known, then σ can be calculated. Within these approximations the invariant distribution for z is exponential in z with parameter σ.

To elucidate equation (28) more fully we define

$$S(\sigma) \equiv \int_{-\infty}^{\infty} L^N(\Lambda^N) e^{-\sigma N\Lambda^N} d\Lambda^N . \tag{29}$$

Remember that S depends on L^N. Solutions of (28) will be solutions of

$$S(\sigma) = 1. \tag{30}$$

Observe that equation (30) has a trivial solution independent of L^N by setting σ=0 in (29). This yields

$$S(0) = \int_{-\infty}^{\infty} L^N(\Lambda^N) d\Lambda^N , \tag{31}$$

and by the definition of normalization (25), we obtain

$$S(0) = 1. \tag{32}$$

Consider now the second derivative of (29),

$$\frac{d^2}{d\sigma^2} S(\sigma) = \int_{-\infty}^{\infty} N^2 \left(\Lambda^N\right)^2 L^N\left(\Lambda^N\right) e^{-\sigma N\Lambda^N} d\Lambda^N \tag{33}$$

This implies that

$$\frac{d^2 S}{d\sigma^2} > 0 \tag{34}$$

because every term in the integral in (33) is positive. We use equations (32) and (34) to make sketches of $S(\sigma)$ in Fig. 2. The five cases in the figure shows all the possible relations that the curve $S(\sigma)$ can have to the horizontal line at S=1. The figure shows that

equation (30) has only one or two solutions. Because we expect the physical solution to depend on L^N the trivial solution $\sigma=0$ is ignored unless the second solution coalesces to $\sigma=0$. The second solution (usually $\sigma\neq0$) depends on L^N and is the physical solution we seek.

One difficulty exists with the exponential form; it is not normalizable. However we can impose two cut-offs on this behavior. For large differences the Taylor expansion in (8) fails; by physical reasoning the separation cannot grow beyond the attractor size, which is assumed to be bounded in z. At small scales the difference noise, ignored between (10) and (21), forces separation of the two systems. Figure 3 shows a histogram of separations taken from computer simulations of a map described later. The horizontal axis displays separation on the scale $z = \ln|r|$. $P(z)$, the probability density of finding the system at separation z, is plotted on a vertical logarithmic scale. Exponential behavior in z will be revealed as a straight line in the figure. The region of interest falls between z=-12 and z=-7; the straight lines in this region show the region of validity of the above analysis. Below z=-12, subsystem asymmetry due to the difference noise causes a dip in probability and destroys the exponential behavior. Above z=-7 the taylor expansion is not valid and the nonlinear terms bring the two subsystems closer to each other keeping them within the attractor size.

If the system is more synchronized than not, the distribution exponent will be negative, and the two systems spend more of their time separated by small distances than large ones. If the exponent is positive, the probability distribution will be weighted toward large separations not small ones. The larger the magnitude of the exponent the stronger the synchronization or desynchronization. One of the three distributions in Fig. 3 is slightly synchronized. The other two curves show that one case is synchronized and the other is unsynchronized. The distribution exponent σ is an excellent continuous measure of the degree of synchronization; a measure that makes intuitive sense because it describes the probability of separation. In addition this exponent closely corresponds to

the idea of a conditional lyapunov exponent. Pikovsky showed and we will also demonstrate that when the conditional lyapunov exponent changes sign, the distribution exponent also changes sign.

Figure 3 exhibits the universal feature of exponential behavior with two cut-offs that seem to be common to many types of maps. Although the previous analysis of invariant distributions uses an unproven assumption that the running average lyapunov exponents Λ^N and the separation z become independent, the analysis seems to apply to many different types of situations. In addition to the piecewise continuous map treated here we have observed exponential distribution of separation, for the logistic map, for maps describing phase locked loops [9], for systems with different noise distributions, and for systems that are fed not with random white noise but with a signal from a deterministic chaotic system. The behavior seems to be fairly universal.

D. Piecewise Linear Map

We introduce a simple piecewise linear map to illustrate some of these ideas,

$$h(x)=\begin{cases} m_+x+\frac{m_-}{2}-\frac{1}{2} & x<-\frac{1}{6} \\ m_-x & -\frac{1}{6}\le x<\frac{1}{6} \\ m_+x-\frac{m_-}{2}+\frac{1}{2} & \frac{1}{6}\le x \end{cases}. \tag{35}$$

For the map (35) to remain continuous the following relationship must hold

$$m_+=\frac{3-m_-}{2}. \tag{36}$$

A plot of the map with m_-=-1 is shown in Fig. 4. We add the white noise ξ_n to the map mod 1 so that w and x stay within the range -1/2 to 1/2. We also add the asymmetric white noise δ_n which has a variance of order 10^{-6}. The mapping equations for the two systems are then

$$\begin{aligned} w_{n+1}&=\left(h(w_n)+\xi_n+\frac{\delta_n}{2}\right)\bmod 1 \\ x_{n+1}&=\left(h(x_n)+\xi_n-\frac{\delta_n}{2}\right)\bmod 1 \end{aligned} \tag{37}$$

We introduce two quantities for future use:

$$\lambda_+ = \ln|m_+| \qquad \lambda_- = \ln|m_-| \tag{38}$$

The synchronization behavior of this map depends mainly on two parameters: the variance of the common noise and the value of the center slope. The two extremes of noise variance can be easily determined analytically.

Without noise the map is stable until the center slope m_- drops below -1. If $|m_-| < 1$, two identical maps without noise will stay synchronized, both with $w=x\approx 0$, until the central fixed point becomes unstable. Any difference between the values of w and x will be entirely due to δ and from (15) will have a variance of approximately $\frac{\langle \delta^2 \rangle}{1-m_-^2}$.

When the fixed point goes unstable the whole map goes unstable and the two points become completely unsynchronized. It is difficult to determine sigma analytically for this low noise case, but it is clear that if it is defined at all the exponent goes from one extreme, of synchronization ($\sigma << 0$), to the other ($\sigma >> 0$), of unsynchronization, very rapidly.

If a full unit of noise is added to the map at every iteration, the map is just as likely to visit any point on the interval -1/2 to 1/2. This is the special case treated by Pikovsky [11]. At each step the map will land on the two outer positively sloped regions with probability $p_+=2/3$ and land in the center region with probability $p_-=1/3$. The lyapunov exponent can be easily determined by using these two probabilities to average the logarithms of the two slopes:

$$\lambda = \tfrac{1}{3}\lambda_- + \tfrac{2}{3}\lambda_+. \tag{39}$$

This full noise forces independence between the current state of the system and any previous states. Because of this independence, (28) holds exactly for $L^1()$, and we can determine sigma analytically. The distribution of the running average for one time step is

$$L^1(\Lambda) = \frac{2}{3}\delta(\Lambda - \lambda_+) + \frac{1}{3}\delta(\Lambda - \lambda_-), \tag{40}$$

where here δ is the dirac delta function. Putting this into (28) gives an equation for sigma

$$1 = p_+ e^{-\sigma\lambda_+} + p_- e^{-\sigma\lambda_-} \tag{41}$$

which can be solved numerically. Both σ and λ cross through zero when $m_- \approx -0.355$. When m_- is greater than this the two maps become synchronized and their trajectories stay mostly close to each other despite their random motions and different initial conditions. As m_- drops below -0.355, the evolution of the two maps is such that the trajectories are more different from each other than similar to each other, i.e. the systems are unsynchronized. Sigma characterizes the continuous transition between synchronized and unsynchronized behavior.

The cases of noise variance that range between no noise and a full unit of noise can be analyzed via (19). We assume that the noise is normally distributed. The gaussian noise and the simple map used in (37) produce an invariant distribution which is approximately a mod 1 gaussian. The analysis determining $\mathsf{E}(g(s)^2)$ must be modified. Calculating the approximate distribution is analogous to (19) except that determining the "variance" of a function on a mod 1 interval is different from determining the variance on the real line, see the appendix.

Once an approximate invariant distribution is known, the lyapunov exponent can be estimated. The probabilities of being in the center negative sloped region, p_-, and the outer positive sloped region, p_+, determine the lyapunov exponent:

$$\lambda = p_+\lambda_+ + p_-\lambda_-. \tag{42}$$

A contour plot of these lyapunov exponents is shown in Fig. 5a for various values of center slope m_- and noise levels. For comparison the lyapunov exponents determined through a computer simulation are also displayed in Fig. 5b. The agreement between the two methods is striking. The transition between synchronized and unsynchronized evolution of the maps occurs along the curve marked zero. The transition happens in a continuous fashion and there is no drastic change as the curve is crossed.

E. Dependence between Adjacent Running Averages

Figure 3 came from the evolution of the map (37). The map serves to illustrate the concept of sigma, and can also elucidate the ideas of the running average lyapunov exponent Λ^N and the dependence between it and the separation z. The distribution exponent is much more difficult to determine analytically than the conditional lyapunov exponent. Unlike the analysis leading to equation (41), we now need to take account of the fact that the process Λ^1 is no longer a white noise process, but that Λ^1 depends on the previous time step. As previously, we average the instantaneous lyapunov exponents over N time steps to obtain a new random process Λ^N. As N increases the running average lyapunov exponents Λ^N become less and less dependent on each other. As N increases in (28) its solution becomes a better and better approximation for sigma.

The distribution of Λ^N can be determined either through numerical simulation or through mapping of the invariant distribution. It is faster computationally to use numerical simulations. Figure 6 gives the predictions of the distribution exponent from (28) for the same amount of common noise and mapping slope but for increasing values of N. It also shows the value of sigma measured from computer simulation (horizontal line). As N increases the prediction becomes closer and closer to the value measured in computer simulations, showing that the running averages become more and more independent of the separation.

A main consequence of the interdependence of instantaneous lyapunov exponents is a shift in variance. The variance of the running average differs from naive predictions, ones which just take into account the instantaneous lyapunov distribution but not the dependence of the instantaneous lyapunov exponent on the previous time step. For map (37) having a noise level of 0.02089 and a center slope $m_c = -0.5$ the probability of having $\Lambda^1 = \lambda_-$ is 0.685 and the probability of having $\Lambda^1 = \lambda_+$ is 0.315. A random variable created from an average of five samples of that random variable would have a variance of 0.0470. However the running average, Λ^5, has a variance 0.0625. The variance of the running

average is larger because once the instantaneous lyapunov exponent has taken on a value, either λ_- or λ_+, it is more likely to take on the same value during the next iteration.

F. Normal Distribution of Running Averages

The distribution of Λ^N for large N approaches a normal distribution, a consequence of the ergodic theorem [12]. The average of Λ^N for large N should be the same as Λ^1 and the variance of Λ^N should decrease proportionally to N. Using this form of a normal distribution in (28) gives

$$1 = \int_{-\infty}^{\infty} \frac{1}{\sqrt{2\pi \upsilon_N}} e^{-\frac{1}{2}\frac{(\Lambda-\lambda)^2}{\upsilon_N}} e^{-N\sigma\Lambda} d\Lambda, \tag{43}$$

where the variance υ is

$$\upsilon = \lim_{N\to\infty} N \operatorname{var}\left(\Lambda^N\right). \tag{44}$$

We integrate (43) to obtain

$$1 = e^{-\lambda N\sigma + \frac{1}{2}\upsilon_N (N\sigma)^2}. \tag{45}$$

Solving for σ we find

$$N\sigma\left(\tfrac{1}{2}\upsilon\sigma - \lambda\right) = 0 \tag{46}$$

and ignore the trivial solution σ=0 to get

$$\sigma = \frac{2\lambda}{\upsilon}. \tag{47}$$

The variance υ is written as a limit to take into account the changes due to dependence mentioned at the end of the last section. The variance υ can be split into two pieces, the variance of the instantaneous lyapunov exponent and a correction due to the dependency between time steps. The variance of the instantaneous lyapunov exponent is $\operatorname{var}\left(\Lambda^1\right)$. The dependency correction is expressed through a diffusion coefficient [13]

$$D = \frac{1}{2} + \frac{\left\langle \Lambda_i^1 \Lambda_{i+1}^1 \right\rangle}{\left\langle \left(\Lambda_i^1\right)^2 \right\rangle} + \frac{\left\langle \Lambda_i^1 \Lambda_{i+2}^1 \right\rangle}{\left\langle \left(\Lambda_i^1\right)^2 \right\rangle} + \ldots \tag{48}$$

with υ expressed as

$$\upsilon = \mathrm{var}(\Lambda^1)2D. \tag{49}$$

The approximation of a normal distribution is best at the maximum of the gaussian and deteriorates toward the tails. The further from zero λ is, the more the tails are emphasized in the calculation for sigma. Consequently this approximation holds best when λ is close to zero.

G. Relation between Lyapunov and Distribution Exponents

Figure 7 shows a plot of σ versus λ for three different noise levels. The plot was generated through computer simulation and each curve is parameterized by m.. Two features are clear from the plot. First σ and λ always change sign together; the graph stays in the 1st and 3rd quadrants and always passes through the origin.

This relationship can be proved through use of the properties of $S(\sigma)$. Recall that $S(0)=1$ and from (34) that S always has positive curvature. The first derivative of S is

$$\frac{dS}{d\sigma} = -\int_{-\infty}^{\infty} N\Lambda^N L^N(\Lambda^N) e^{-\sigma N\Lambda^N} d\Lambda^N. \tag{50}$$

We evaluate (50) at $\sigma=0$ to obtain

$$\left.\frac{dS}{d\sigma}\right|_{\sigma=0} = -\int_{-\infty}^{\infty} N\Lambda^N L^N(\Lambda^N) d\Lambda^N. \tag{51}$$

From

$$\lambda = \int_{-\infty}^{\infty} \Lambda^N L^N(\Lambda^N) d\Lambda^N \tag{52}$$

we have that

$$\left.\frac{dS}{d\sigma}\right|_{\sigma=0} = -N\lambda. \tag{53}$$

A negative lyapunov exponent selects Figs. 2a and 2d as the only possibilities for the relationship between $S(\sigma)$ and the horizontal line at 1, because through equation (53) the slope of $S(\sigma)$ through 0 must be positive. So the second solution, if it exists, must be less than zero, just like the lyapunov exponent. Similarly, if the lyapunov exponent is

positive, the slope must be negative, Figs. 2b and 2e are the only possibilities, and the second solution must be positive.

The second feature of Fig. 7 is that the transition through the origin happens abruptly for low noise levels and gradually for large noise levels. The slope of the line at zero quantifies the rate of transition from synchronized to unsynchronized behavior. It can be determined analytically from (47). Using expressions for λ, Λ^1 and υ

$$\lambda = p_+\lambda_+ + p_-\lambda_-, \tag{54}$$

$$\left\langle \left(\Lambda^1\right)^2 \right\rangle = p_+\lambda_+^2 + p_-\lambda_-^2, \tag{55}$$

$$\upsilon = \mathrm{var}(\Lambda^1)2D = \left(\left\langle \left(\Lambda^1\right)^2 \right\rangle - \lambda^2\right)2D = -(\lambda-\lambda_+)(\lambda-\lambda_-)2D \tag{56}$$

and substituting into (47) gives

$$\sigma = \frac{-2\lambda}{(\lambda-\lambda_+)(\lambda-\lambda_-)2D}. \tag{57}$$

The derivative of (57) with respect to λ is

$$\frac{d\sigma}{d\lambda} = \frac{2\left(\lambda^2(1-\frac{d(\lambda_+ + \lambda_-)}{d\lambda}) - \lambda_-\lambda_+ + \lambda\lambda_+\frac{d\lambda_-}{d\lambda} + \lambda\lambda_-\frac{d\lambda_+}{d\lambda}\right)}{(\lambda-\lambda_-)^2(\lambda-\lambda_+)^2 2D}. \tag{58}$$

Evaluating (58) at λ=0 yields

$$\left.\frac{d\sigma}{d\lambda}\right|_{\lambda=0} = \frac{-2}{\lambda_-\lambda_+ 2D}. \tag{59}$$

Table I below shows a comparison between measured values and predicted values of $\left.\frac{d\sigma}{d\lambda}\right|_{\lambda=0}$. The diffusion coefficient D defined in (48) was calculated using computer simulations.

III. CONCLUSIONS

We have shown that a good way to quantify the degree of synchronization is through use of the distribution exponent σ. This has many connections to an intuitive idea of synchronization and is also relatively easy to measure. We have explored a simple piecewise linear map to examine σ and λ and their relationship in synchronization transition regions. We have also observed and explained differences in the transition between synchronized and unsynchronized behavior for differing levels of noise.

ACKNOWLEDGMENTS

We would like to acknowledge Maria de Sousa Vieira who first brought Pikovsky's paper to our attention, and has helped edit this paper. This work was partially supported by ONR grants N00014-95-I-0361 and N00014-89-J-1097, and by NSF grant PHY-9505621.

APPENDIX

All the distributions dealt with in this paper have zero mean so that their variance and second moment are completely equivalent. The integral expression for measuring the second moment over the real line is

$$\text{SecondMoment}(g(x)) = \int_{-\infty}^{\infty} x^2 g(x) dx. \tag{A1}$$

This is useful in equations (14) and (19) because the sum of variances of two independent random variables defined on the real line equals the variance of the sum of the same two random variables. However "second moment" on the circle defined by a truncated version of equation (A1)

$$\text{SecondMoment}(g(x)) = \int_{-1/2}^{1/2} x^2 g(x)dx \tag{A2}$$

does not have the distributive property for the addition of random variables on the circle. For this situation it is more useful to determine the second moment from the second derivative evaluated at the zero of the fourier transform of a function

$$\text{SecondMoment}(g(x)) = \int_{-\infty}^{\infty} x^2 g(x)dx = -\frac{d^2}{d\omega^2}\int_{-\infty}^{\infty} e^{-i\omega x} g(x)dx\Big|_{\omega=0} = -\frac{d^2}{d\omega^2}G(\omega)\Big|_{\omega=0}. \tag{A3}$$

Our definition for "second moment" on a circle will be analogous to this. Determine the fourier series for a function on a circle and estimate the second derivative of the series at the origin in Fourier space from a number of elements in the series. The analogy is illustrated in Fig. A1 where we show a function defined in real space and its fourier transform and a function defined in periodic space and its fourier series.

A good account of estimates for the second derivative can be found in [14]. We use the seven point formula:

$$\text{Var}() \approx \tfrac{4}{360}x_{-3} + \tfrac{-54}{360}x_{-2} + \tfrac{540}{360}x_{-1} + \tfrac{-980}{360}x_0 + \tfrac{540}{360}x_1 + \tfrac{-54}{360}x_2 + \tfrac{4}{360}x_3. \tag{A4}$$

This definition works well producing accurate results as shown in Fig. 5.

Table I Comparison of the values of $\left.\frac{d\sigma}{d\lambda}\right|_{\lambda=0}$ measured through computer simulations and predicted from equation (59) for a various common noise variances. The diffusion coefficient was calculated through computer simulations.

	Noise variance	Diffusion coefficient	$\left.\frac{d\sigma}{d\lambda}\right\|_{\lambda=0}$ Prediction	$\left.\frac{d\sigma}{d\lambda}\right\|_{\lambda=0}$ Simulations
Large Noise	0.069773	1.269	3.64	3.53
Medium Noise	0.020895	1.415	7.27	7.08
Low Noise	0.002315	1.452	40.7	36.8

FIGURE CAPTIONS

FIG. 1a. Invariant distribution of a piecewise linear map $h(x)$ with additive noise. The map is 0 from x=-1 to x=1 and has slope 1/2 everywhere else. The noise is white noise gaussianly distributed with unity variance. The computer simulation and the self consistent prediction are indistinguishable from each other.

FIG. 1b. The error between a distribution estimated from a computer simulation of this map and a gaussian distribution with variance calculated using equation (19). The simulation was run through 50,000,000 iterations and sorted into overlapping bins of width x=0.6.

FIG. 2. Five different possible cases for the shape of the curve $S(\sigma)$ given in (29). Solutions to (30) appear as intersections between the curve and the line σ=1 are also plotted. In (a), (b), and (c) there is only one solution to (30) and the physical solution has gone to minus infinity, infinity, and zero respectively; (d) and (e) each show two solutions to (30); the physical solution in (d) is negative while the physical solution in (e) is positive.

FIG. 3. $P(z)$, the probability density, is plotted on a logarithmic scale versus the separation $z = \ln|r|$. ($P(z)dz$ is the probability of finding the two systems described by the mapping (37) between the range of separations z and $z+dz$) The common noise is gaussianly distributed. The difference noise is gaussianly distributed with variance 10^{-6}. There are three different maps shown. The synchronized map has center slope -0.1 and common noise variance 0.0698. The map that is barely synchronized has center slope -0.951 and common noise variance 0.00231. The unsynchronized map has center slope -0.5 and common noise variance 0.0698.

FIG. 4. A plot of the function h in (35) with m_-=-1 and m_+=2.

FIG. 5. Two contour plots of conditional lyapunov exponent in the parameter space of noise variance ξ and center slope m_- of the piecewise linear map. The noise is gaussianly distributed with a variance indicated on the vertical scale. The contour lines are spaced every 0.25. Plot (a) comes from analysis; plot (b), from simulation.

FIG. 6. Plot of the prediction for sigma produced by the distribution of Λ^N for increasing N. The measurements were taken at a large noise level with a gaussian variance of 0.069 and a center slope of the piecewise linear map of -0.1.

FIG 7. Plot of the distribution exponent versus the lyapunov exponent for three different noise levels. The large, medium, and low noise levels used had variances of 0.0698, 0.0209, and 0.002315 respectively.

FIG. A1a. Plot of the real line hat function. It is non zero only from -1/4 to 1/4 and is defined over the whole real line.

FIG. A1b. Plot of the hat function in fourier space, $\frac{\mathrm{Sin}(\frac{\omega}{4})}{\frac{\omega}{4}}$. It is defined over the real line and its second derivative at zero is equal to the variance of the hat function $\frac{d^2}{d\omega^2}\left(\frac{\mathrm{Sin}(\frac{\omega}{4})}{\frac{\omega}{4}}\right)\Big|_{\omega=0}$

FIG. A1c. Plot of the periodic hat function. Again the function is non zero from -1/4 to 1/4, but now it is only defined from -1/2 to 1/2.

FIG. A1d. Plot of the periodic hat function in fourier space, $\frac{\mathrm{Sin}(\frac{\pi}{4})}{\frac{\pi}{4}}$. It is only defined over the integers, and the estimate of the second derivative at n=0 is defined to be the variance of this periodic function.

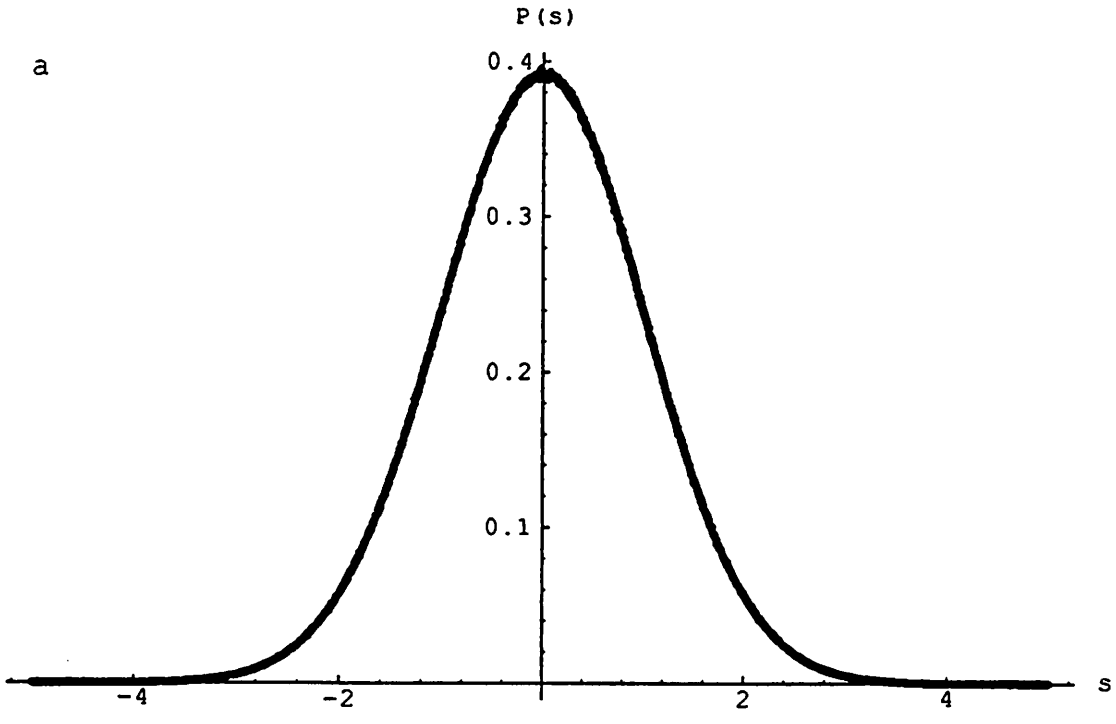

Figure 1a

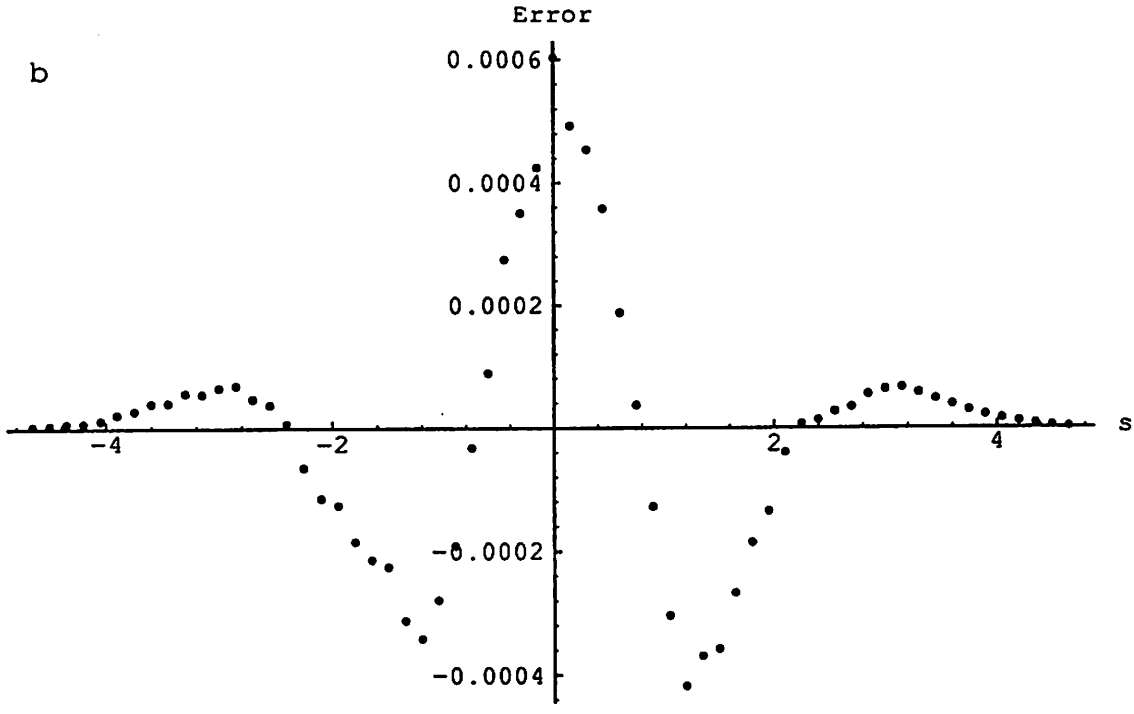

Figure 1b

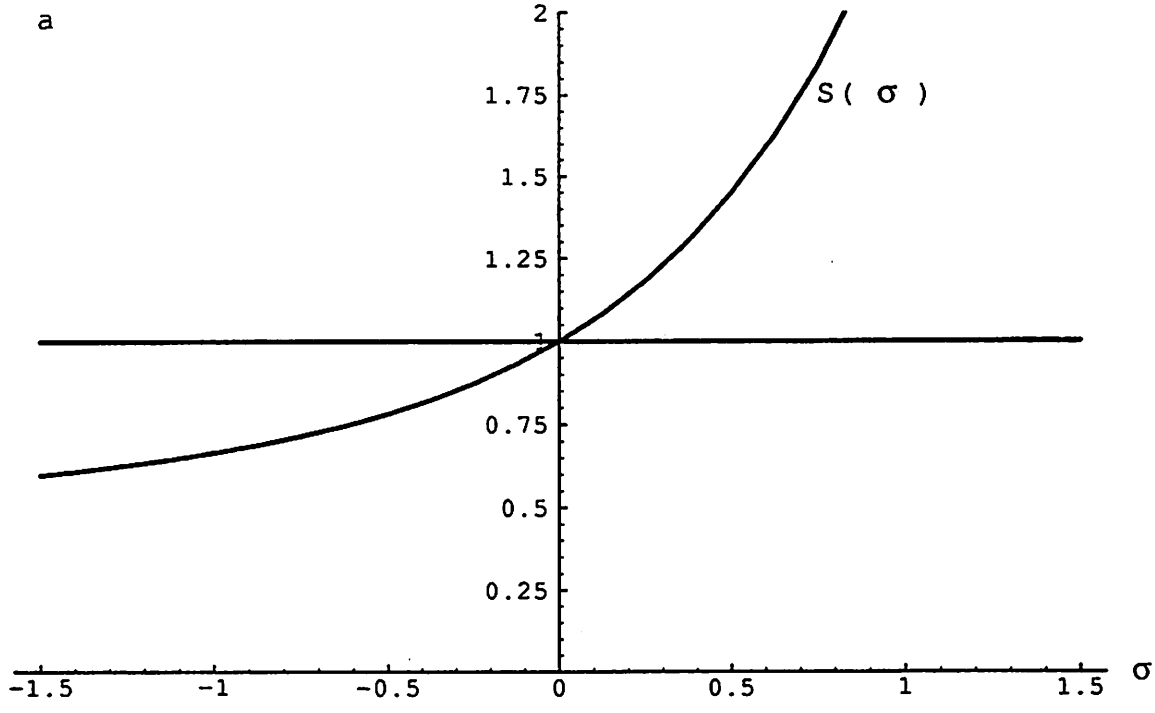

Figure 2a

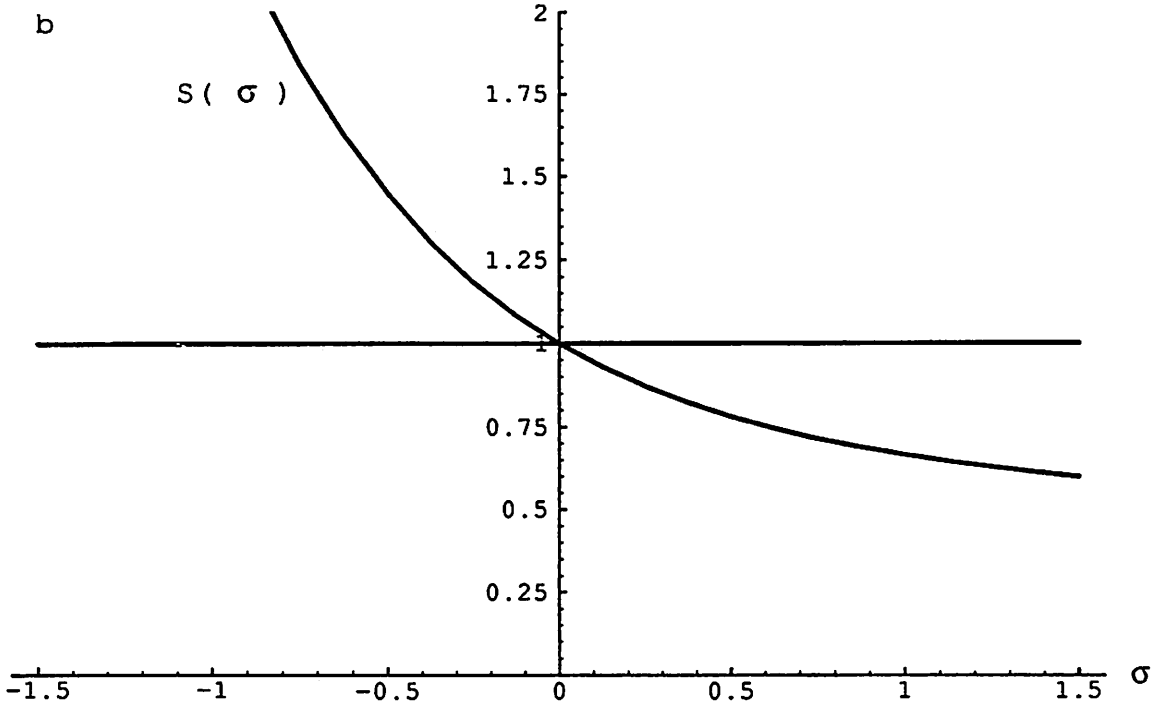

Figure 2b

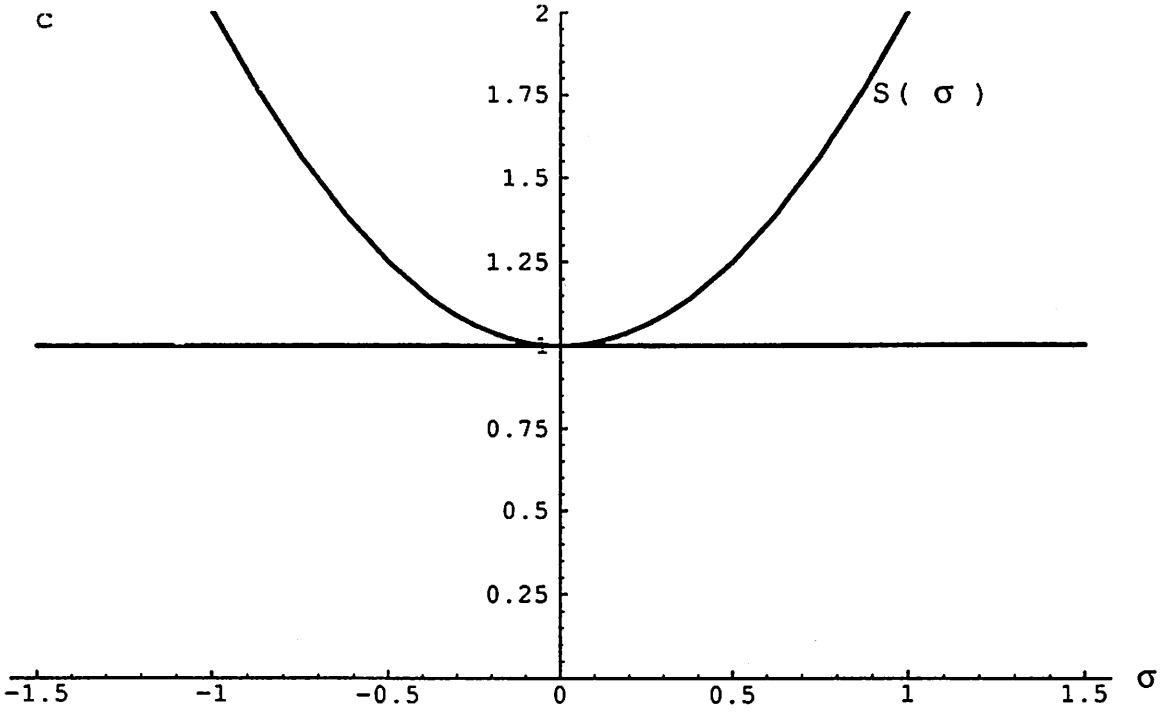

Figure 2c

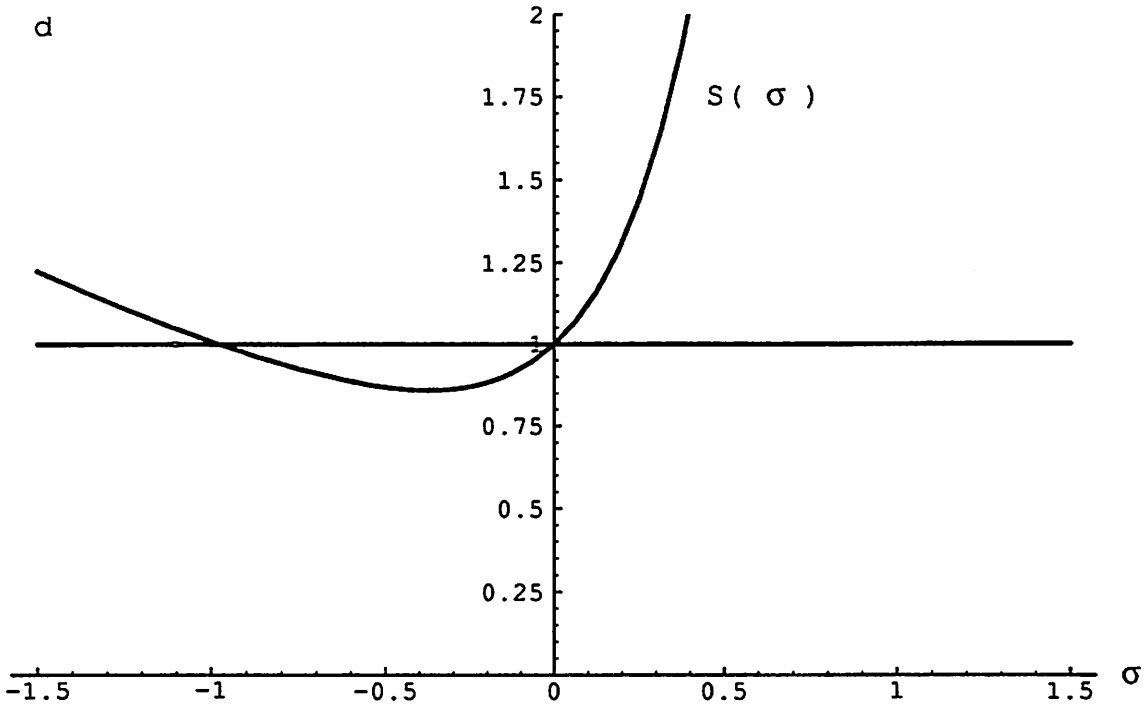

Figure 2d

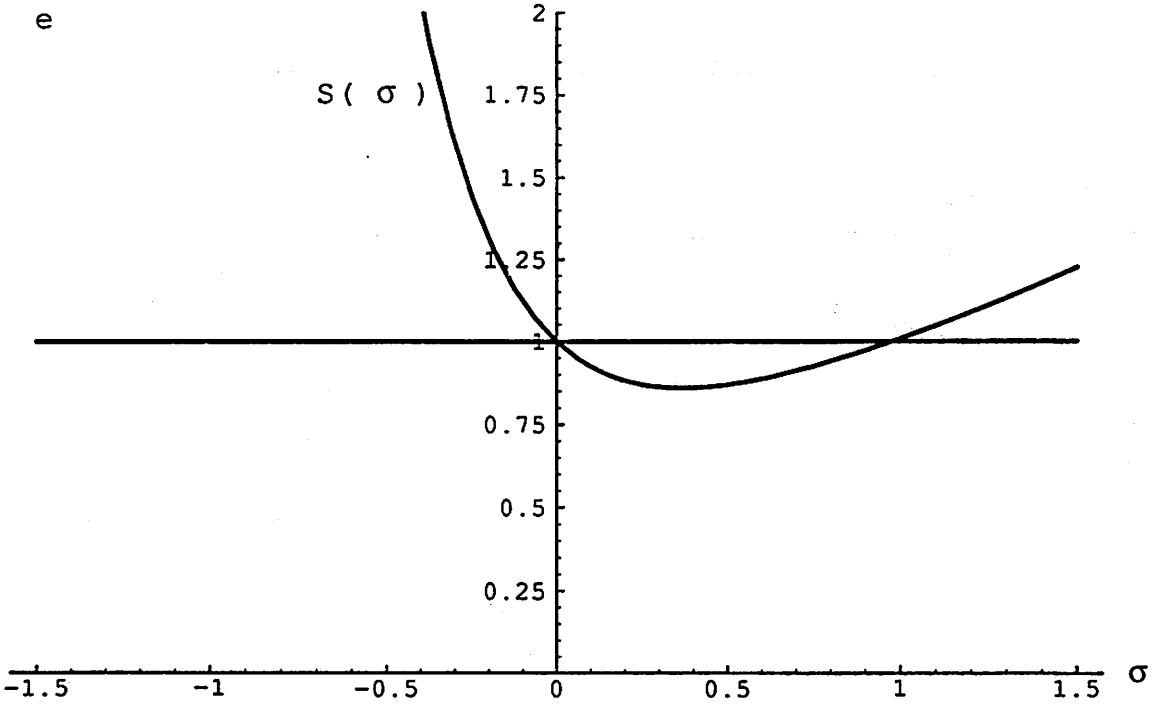

Figure 2e

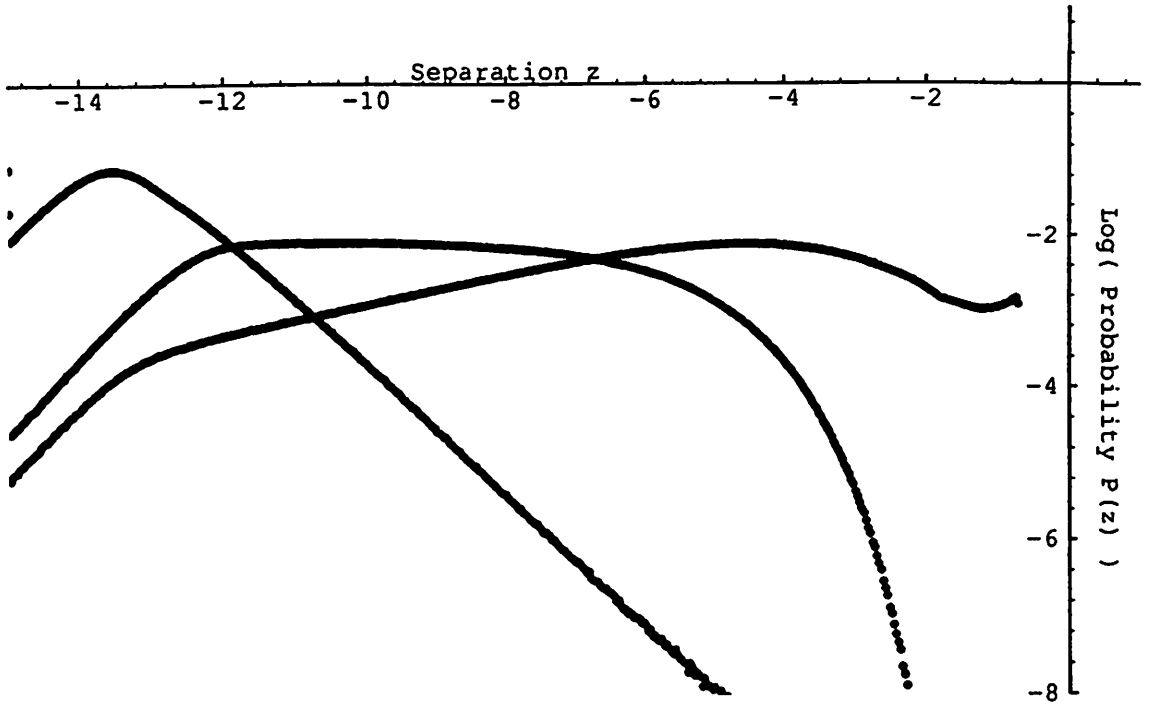

Figure 3

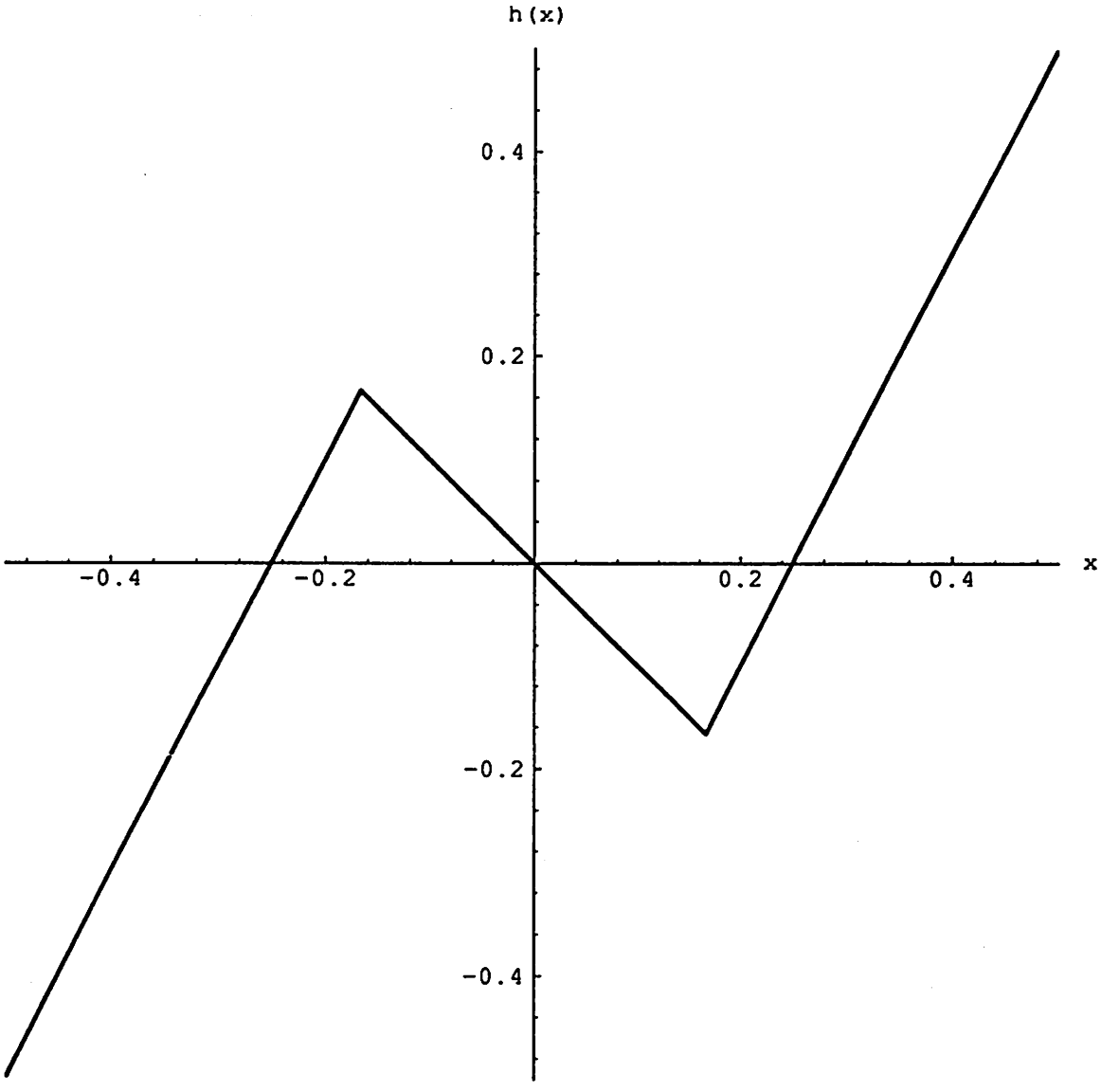

Figure 4

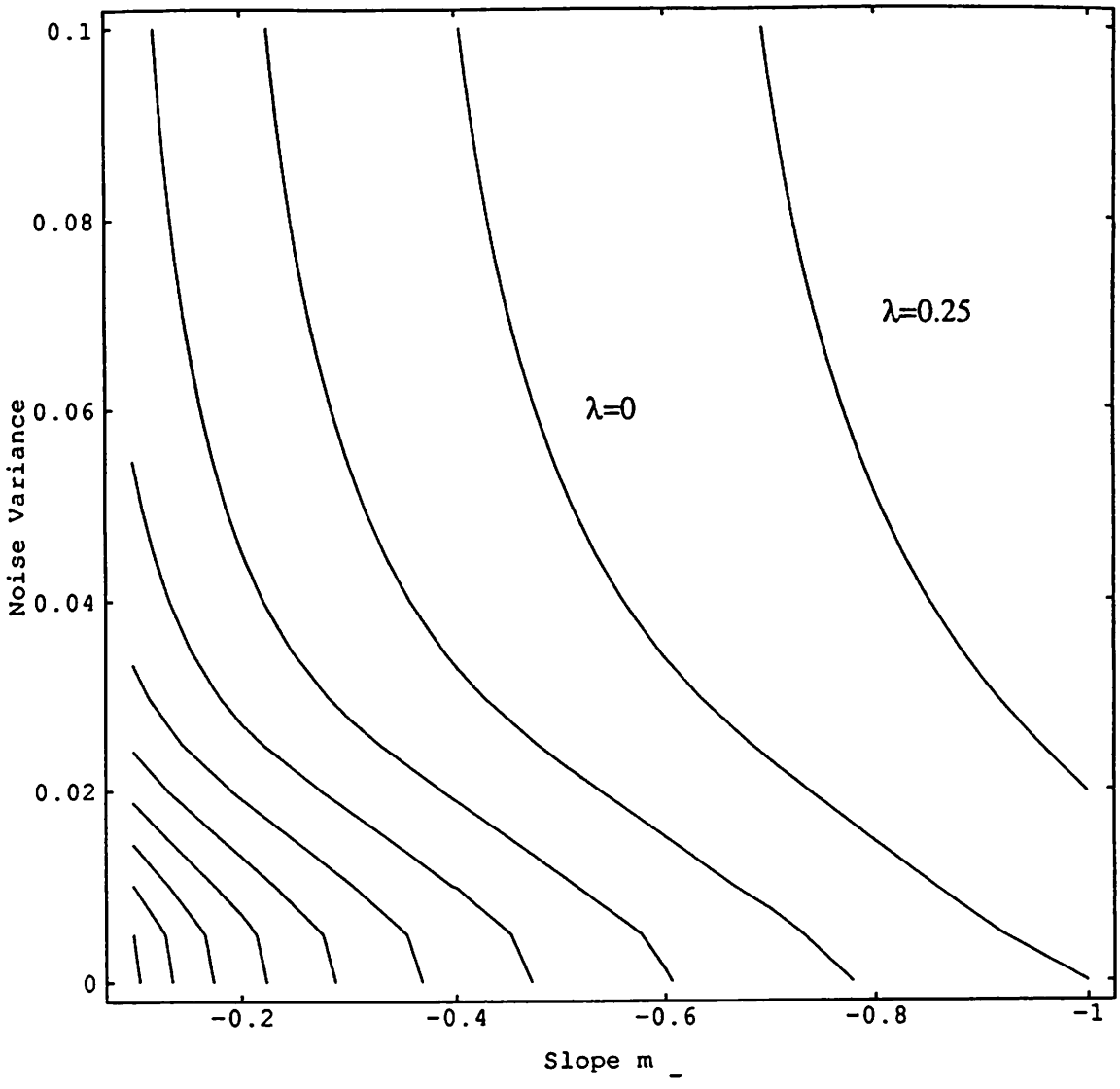

Figure 5a

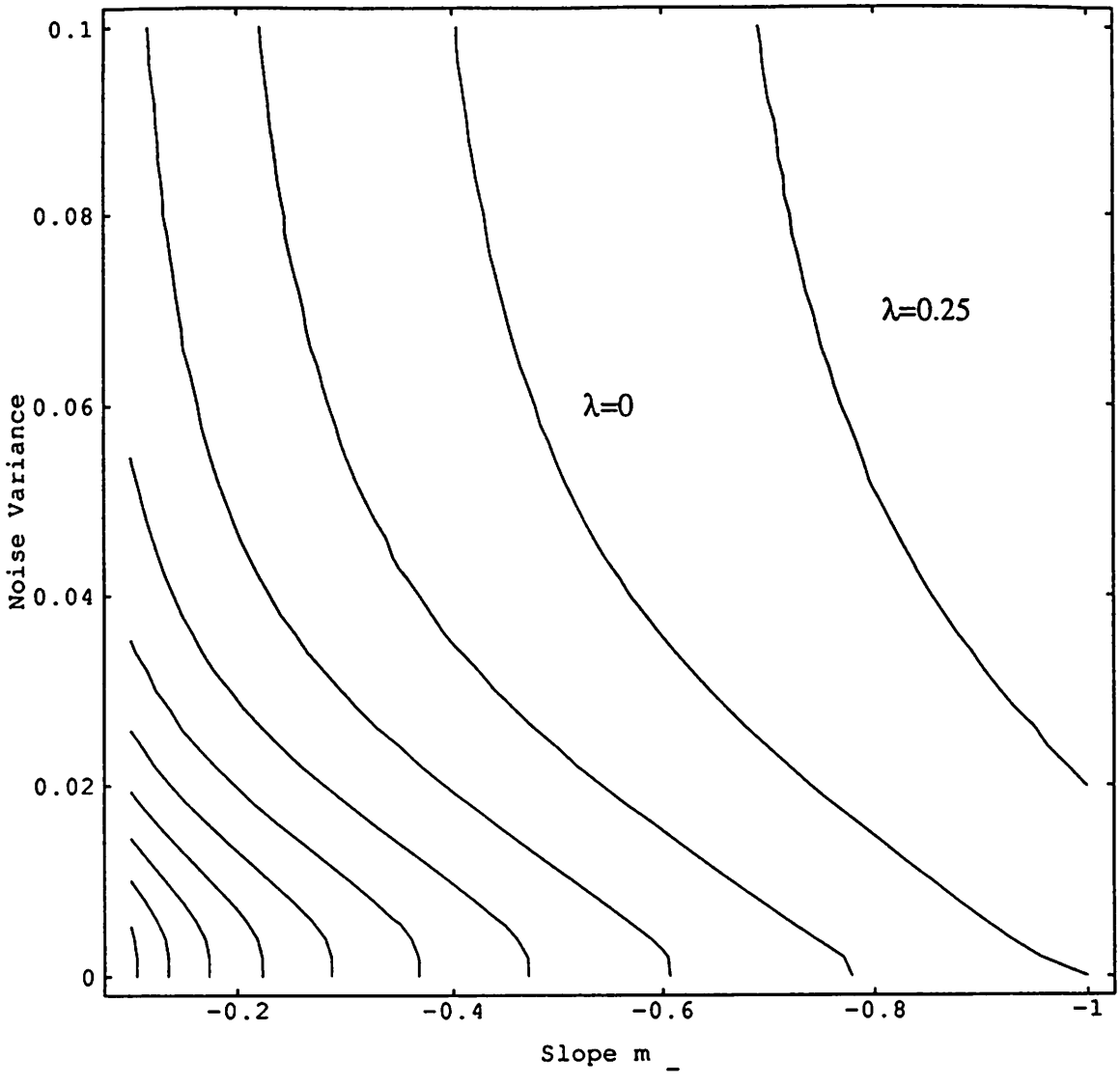

Figure 5b

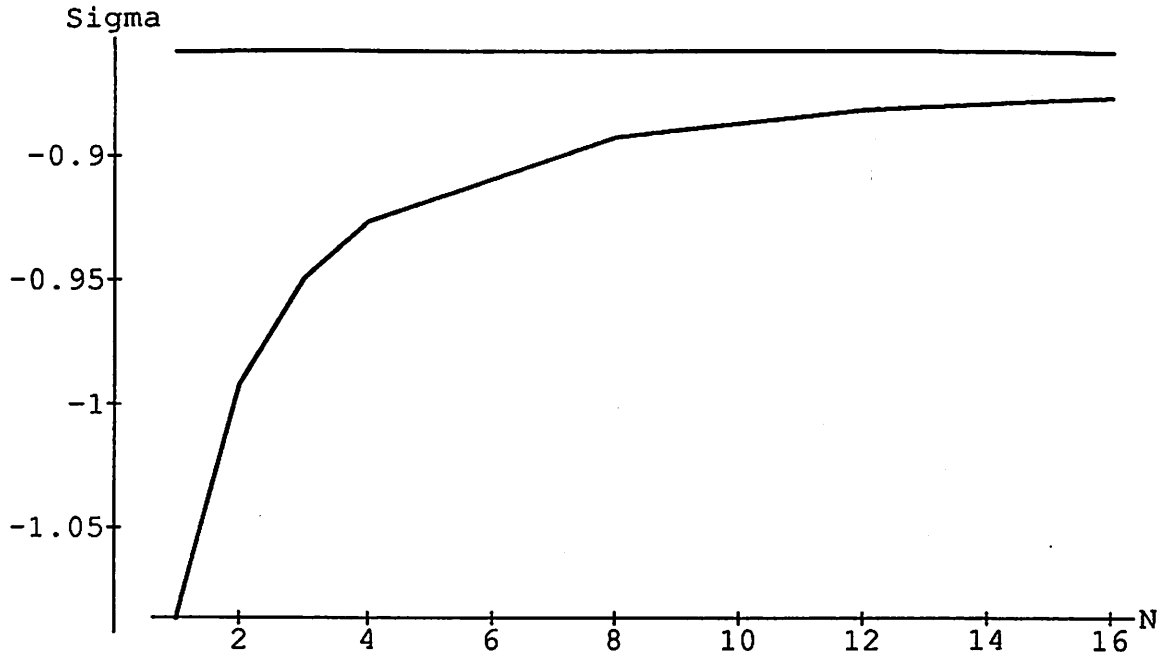

Figure 6

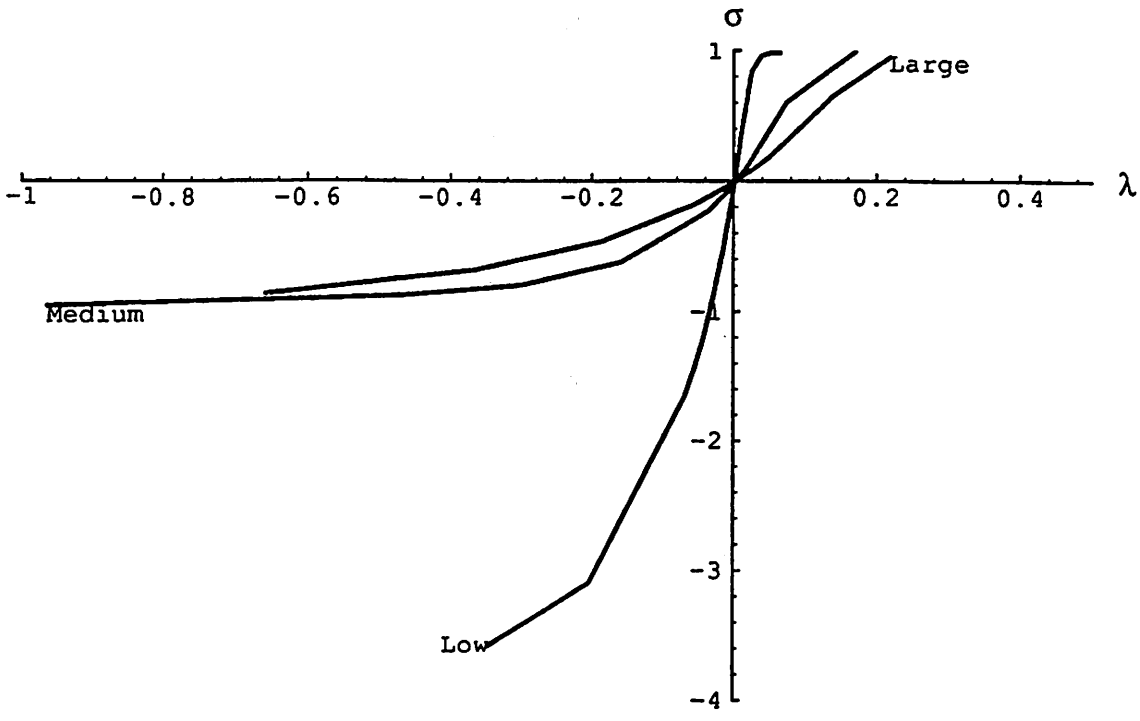

Figure 7

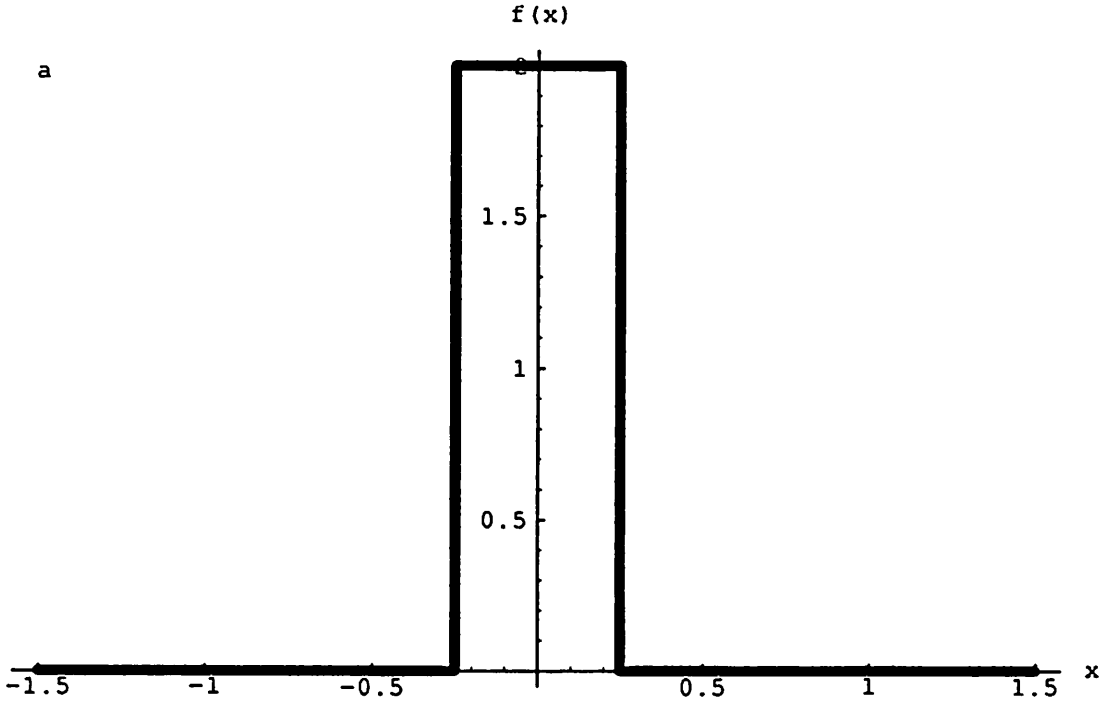

Figure A1a

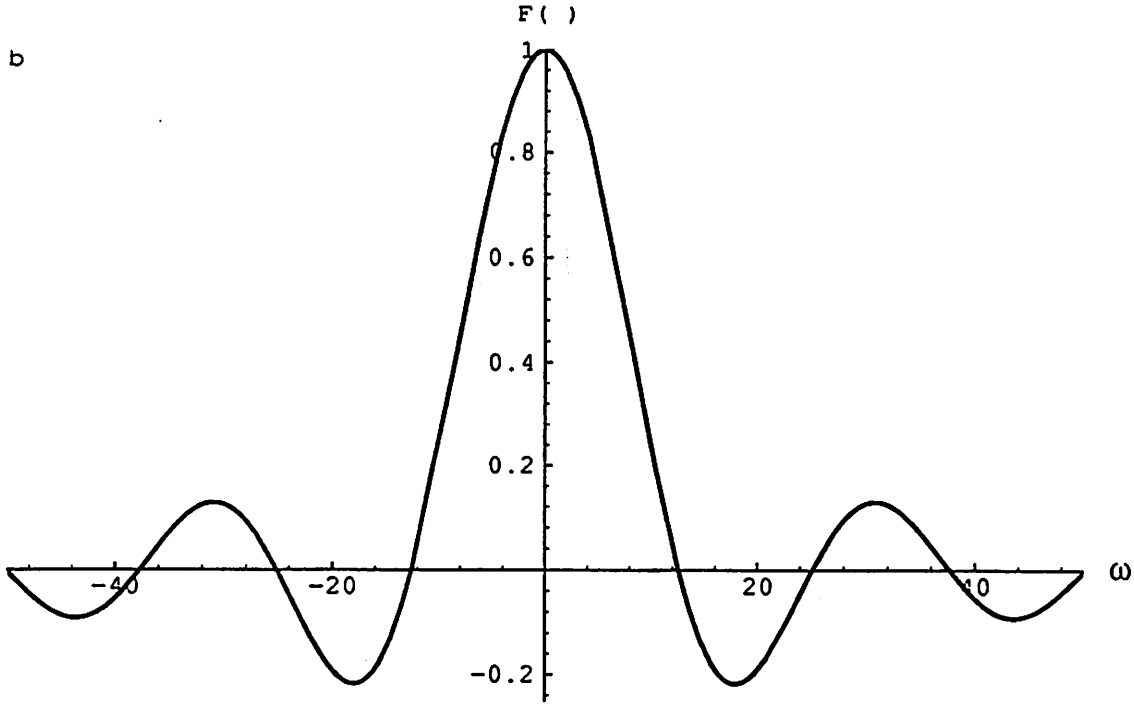

Figure A1b

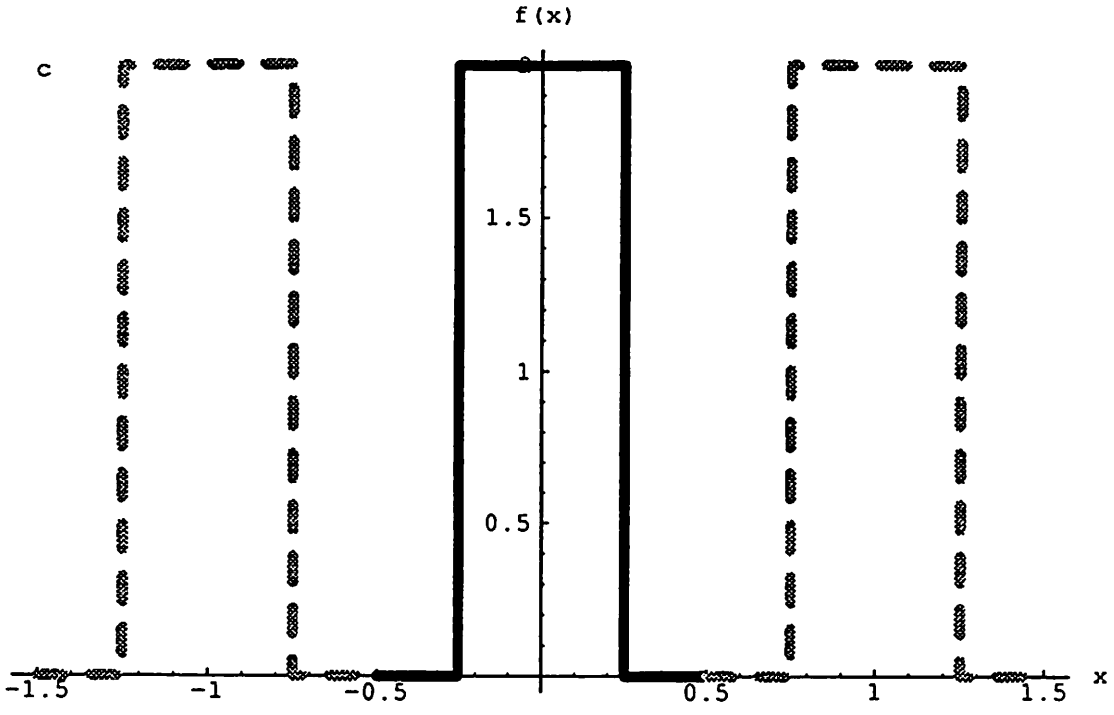

Figure A1c

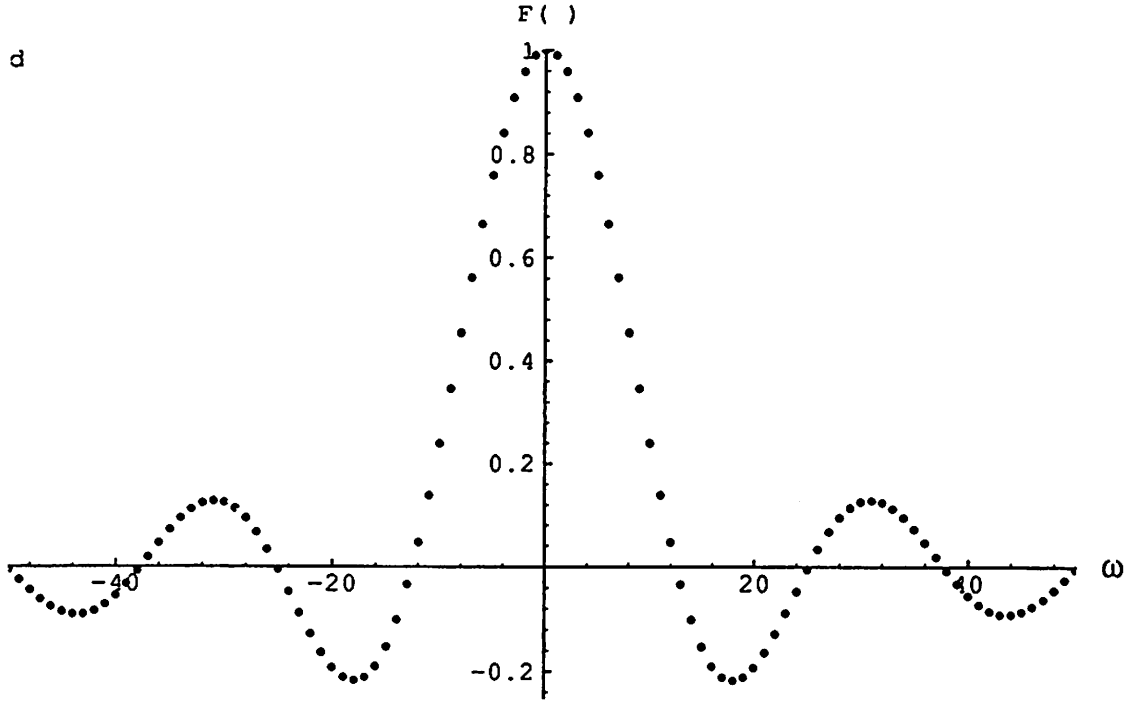

Figure A1d

References

[1] L. M. Pecora and T. L. Carroll, Phys. Rev. A **44**, 2374 (1991)

[2] H. Fujisaka and T. Yamada, Prog. Theor. Phys. **69**, 32 (1983)

[3] V. S. Afraimovich, N. N. Verichev, and M. I. Rabinovich, Izv. Vysch. Uchebn. Zaved. Radiofiz, **29**, 1050 (1986)

[4] A. Maritan and J. R. Banavar, Phys. Rev. Lett. **72**, 1451 (1994)

[5] A. Pikovsky, Phys. Rev. Lett. **73**, 2931 (1994)

[6] A. Maritan and J. R. Banavar, Phys. Rev. Lett. **73**, 2932 (1994)

[7] H. Herzel and J Freund, Phys. Rev. E **52**, 3238 (1995)

[8] F. M. Collier and C. A. Desoer, Linear System Theory, (Springer-Verlag, NY, 1991).

[9] M. de Sousa Vieira, et al, Int. J. Bifurcation Chaos, **2**, 645 (1992)

[10] U. Parlitz, et al, Int. J. Bifurcation Chaos, **2**, 973 (1992)

[11] A. S. Pikovsky, Phys. Letters A, **165**, 33 (1992)

[12] R. Durrett, *Probability: Theory and Examples*, (Wadsworth Brooks/Cole Publishing Co., Pacific Grove,1991).

[13] H. Fujisaka, Prog. Theor. Phys., **70**, 1264 (1983)

[14] S. Yakowitz and F. Szidarovsky, *An Introduction to Numerical Computations*, (Macmillan Publishing Co., NY, 1986).